ELSEVIER

PII: S0144-8617(96)00106-3

Carbohydrate Polymers 30 (1996) 83–93

0144-8617/96/$15.00 + .00

Small angle X-ray characterization of gellan gum containing a high content of sodium in aqueous solution

Yoshiaki Yuguchi,[a] Mitsuru Mimura,[a] Hiroshi Urakawa,[a] Shinichi Kitamura,[b] Shigeru Ohno[c] & Kanji Kajiwara[a]*

[a]*Faculty of Engineering & Design, Kyoto Institute of Technology, Kyoto, Sakyo-ku, Matsugasaki 606, Japan*
[b]*Faculty of Agriculture, Kyoto Prefectural University, Kyoto, Sakyo-ku, Shimogamo 606, Japan*
[c]*Japan Synchrotron Radiation Research Institute (JASRI), Hyogo, Ako-gun, Kamigohri, Kanaji 678-12, Japan*

A temperature dependence of small-angle X-ray scattering (SAXS) profiles was observed from the aqueous solutions of bacterial polysaccharide gellan gum at various concentrations. The sample is a water-soluble sodium salt type and is provided by Kelco Division of Merk & Co. for use by the Gellan Gum Working Party organized by the Gel Research Group of the Society of Polymer Science and Technology. The cross-sectional radius of gyration $R_{G,c}$ evaluated by cross-sectional Guinier plots indicates that gellan gum consists mainly of single chains at higher temperatures. On cooling, $R_{G,c}$ was observed to increase to the value corresponding to the gellan double helix at lower concentrations when no gelation takes place. At higher concentration where a gel is formed, a much larger $R_{G,c}$ was obtained, suggesting the further association of double helices. The observed SAXS profiles were analyzed in terms of the broken rod-like model where the rod thickness and the interference due to the repulsive interaction between domains was taken into account. The calculated scattering function describes well the SAXS profile from gellan gum aqueous solutions. Copyright © 1996 Elsevier Science Ltd

INTRODUCTION

Gellan gum is an extracellular polysaccharide produced by *Pseudomonas elodea*, and is composed of tetrasaccharide repeat units: 1,3-linked β-D-glucose, 1-4-linked β-D-glucuronic acid, 1,4-linked β-D-glucose and 1,4-linked α-L-rhamnose (Jansson *et al.*, 1983). Gellan gum forms a thermoreversible gel upon cooling (Crescenzi *et al.*, 1986), but its gelling mechanism is not yet fully understood. The formation of the ordered conformation (probably a double-stranded helix) and subsequent alignment of the ordered regions are said to be responsible for gel formation (Carroll *et al.*, 1983). The structure of the gellan gum chains was observed directly by electron microscopy (Stokke *et al.*, 1993). The present work aims to specify the structural characteristics of gellan gum in the sol and gel states in aqueous solution by means of small-angle X-ray scattering (SAXS). The study was carried out with the gellan gum sample distributed among the working party organized by the Gel Research Group of the Society of Polymer Science and Technology, Japan (A special issue of Food Hydrocolloids, 1993). The new sample was prepared so as to be soluble in cold water by transforming to the sodium salt type, and its metal contents were different from the previously distributed sample which had a high content of potassium and calcium. Since the gelling characteristics depend on the type and concentration of counter ions (Grasdalen & Smidsød, 1987; Milas *et al.*, 1990), the new sodium-salt-type gellan sample is expected to reveal a new aspect of the gelling mechanism. This material had a weak gelling ability compared with the sample containing higher levels of potassium and calcium.

*Corresponding author.

EXPERIMENTAL

Sample preparation

Gellan gum sample was provided by Kelco Division of Merk & Co. Inc., CA, USA. Metal contents were

analyzed as Na 3.03%, K 0.19%, Ca 0.11% and Mg 0.02%. The gellan sample was used as supplied without further treatment. The powdered gellan was weighed directly into a weighing bottle, and water added to give concentrations of $C_p = 1.0$, 1.5, 2.9, 5.7wt%, left to swell in warm water for several hours, and then dissolved by heating the solution up to 80°C. The solutions were placed in the thermostated cells for SAXS measurements after filtration through filters of 0.8μm pore size at high temperature.

Small-angle X-ray scattering

The SAXS measurements were carried out at BL-10C of the Photon Factory in the National Laboratory for High Energy Physics, Tsukuba, Japan. An incident X-ray from synchrotron radiation was monochromatized to $\lambda = 1.49$Å with a double-crystal monochrometer, and then focused to a focal point with a bent focusing mirror. The scattered X-rays were detected by a one-dimensional position sensitive proportional counter (PSPC) positioned at the distance of about 1m from the sample holder. A flat sample cell of 0.2cm path-length made of glass with windows of quartz plates of 20μm thickness was used. The cell was thermostated by circulating water of a constant temperature through the cell holder. The solutions were injected into the cell at a fixed temperature for several tens of minutes prior to the SAXS measurement. The SAXS intensities were accumulated for 115–600s in order to assure enough statistical precision without degrading gellan gels by X-ray irradiation. The scattering intensities were corrected for the variation in the incident X-ray flux by monitoring with an ion chamber in front of the cell holder and for the X-ray absorption of solutions by measuring the incident and transmitted X-ray intensities. The excess scattering intensities were evaluated by subtracting the scattering intensities of the solvent from those of the gellan solutions.

RESULTS AND DISCUSSION

Figure 1 exhibits the SAXS results from the gellan aqueous solution at 60°C (80°C for $C_p = 5.7\%$) and 10°C (the concentrations are shown in the figure). The SAXS profile changed drastically with decreasing temperature. The solutions of $C_p = 2.9$ and 5.7% form a gel at 10°C, but no gelation takes place at the other lower concentrations. Here the gel is defined as the state where the solution will not flow on inclining the solution container. The scattered intensity $I(q)$ increases by cooling, where $I(q)$ denotes the excess scattered intensity with respect to water and q is the magnitude of scattering vector given by $4\pi\sin\theta/\lambda$ with θ and λ being a half of the scattering angle and the wavelength of incident X-ray, respectively. A weak peak appears around $q = 0.05$–0.07Å^{-1} on cooling due to electrostatic interaction in the solutions of $C_p = 1.0$–2.9%, while at higher concentration $C_p = 5.7\%$ a corresponding peak disappears. Taking the example of the 1.5% solution, the cross-sectional radius of gyration $R_{G,c}$ was found to increase from 3.0Å at 60°C to 4.0Å at 10°C as indicated by cross-sectional Guinier plots (Fig. 2) according to the formula:

$$qI(q) \sim \exp(-R_{G,c}^2 q^2/2) \quad (1)$$

The cross-sectional radius of gyration at 10°C ($R_{G,c} = 4.0$Å) corresponds to the cross-sectional radius of $R_c = 5.7$Å when a circular cross-section of homogeneous density is assumed. This value is equal to the cross-sectional radius of the gellan double helix (Dentini *et al.*, 1988), and a smaller value of $R_{G,c}$ at 60°C is thought to indicate a single chain structure or the mixture of single and double chains. Similarly $R_{G,c}$ was evaluated at various concentrations as summarized in Table 1.

The gellan gum molecular models (Chandrasekaran *et al.*, 1988) of a double helix and a single helix were constructed by linking 5 tetrasaccharide repeat units, and the scattering profiles from the models were calculated according to the Debye formula (see, for example, Glatter, 1982), as shown in Fig. 3. The cross-sectional radius of gyration was evaluated as 3.4 or 2.6Å for a double helix or a single helix, respectively, from the cross-sectional Guinier plots (Fig. 3). In the following discussion, these values are compared with the values estimated from the observed scattering profiles. At higher temperatures, the value of $R_{G,c}$ lies in the range of 1.8–3.0Å, suggesting that the system is composed mainly of single chains and may contain a small portion of double-stranded chains. The lower value than 2.6Å may indicate a further unfolding from a single helix to a random coil. Cooling causes double-helix formation, but no gelation takes place at lower concentrations ($C_p = 1.0$, 1.5%). At higher concentrations ($C_p = 2.9$, 5.7%) where a gel is formed, a larger $R_{G,c}$ value than 4.0Å is evaluated at 10°C, and the result is attributed to the subsequent alignment of gellan double helices.

Here two components of cross-sectional radii were found to exist in the solutions of higher concentrations in the gel state. This confirms our previous conclusion that the subsequent side-by-side association of double helices promotes gelation of gellan (Yuguchi *et al.*, 1993).

The relative linear mass density at 10°C with respect to 60°C (or 80°C), $M_L(10°C)/M_L(60°C)$ can be estimated by comparing the limiting value of $qI(q)$ at $q \to 0$ in each state, which is proportional to the linear mass density of gellan chains. These values were found to be 2 at lower concentrations ($C_p = 1.0$, 1.5%) and larger than 2 at higher concentrations ($C_p = 2.9$, 5.7%). The results confirm the further association of double helices at higher concentrations in the gel state. However at lower

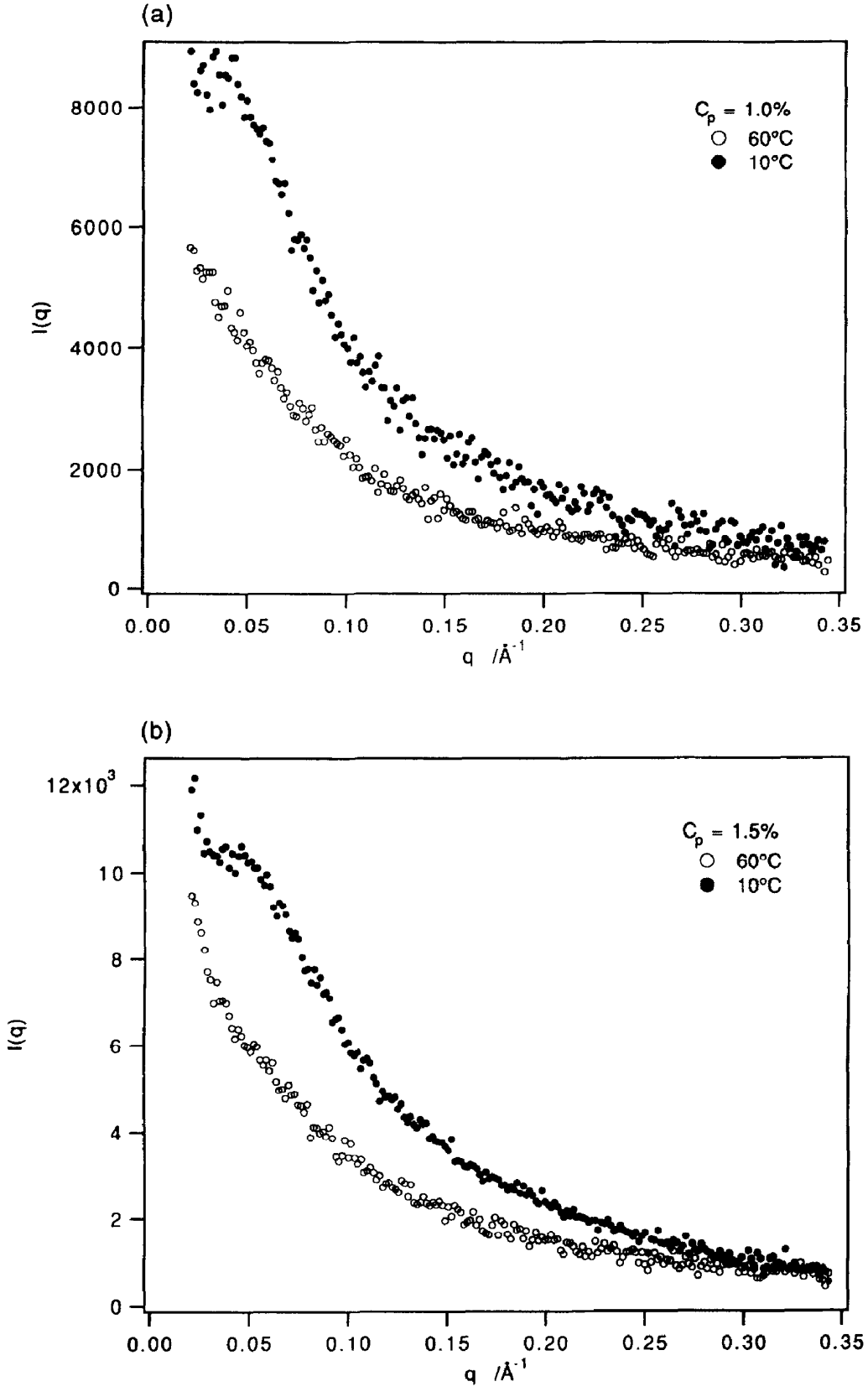

Fig. 1. Small-angle X-ray scattering profiles from gellan gum aqueous solutions. The concentrations and temperatures are indicated in the figure.

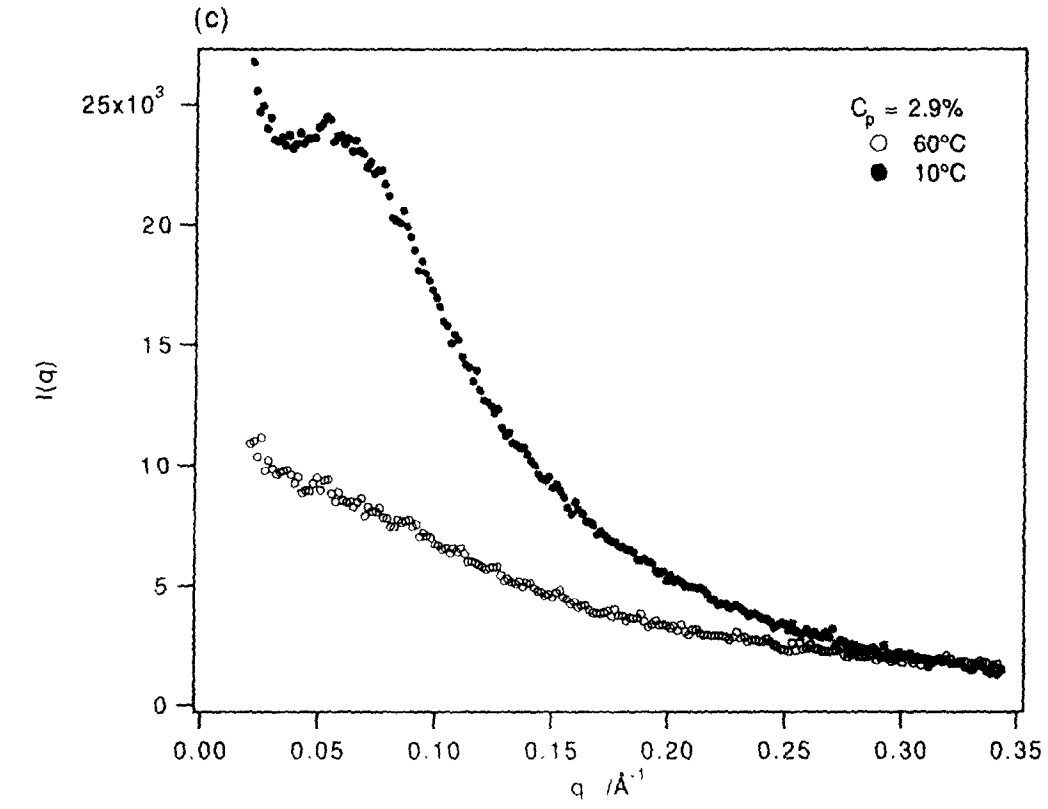
(c)
25x10^3
20
15
10
5
0
I(q)
C_p = 2.9%
60°C
10°C
0.00
0.05
0.10
0.15
0.20
0.25
0.30
0.35
q /Å^-1

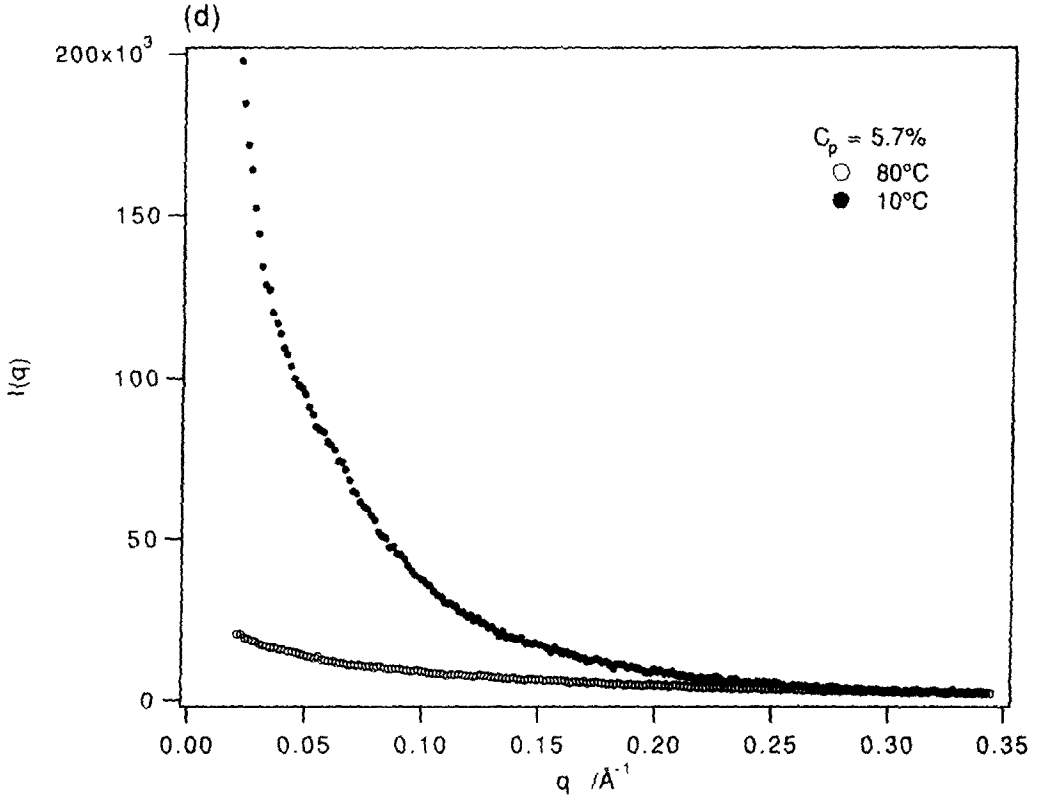
(d)
200x10^3
150
100
50
0
I(q)
C_p = 5.7%
80°C
10°C
0.00
0.05
0.10
0.15
0.20
0.25
0.30
0.35
q /Å^-1

Fig. 1. *Contd.*

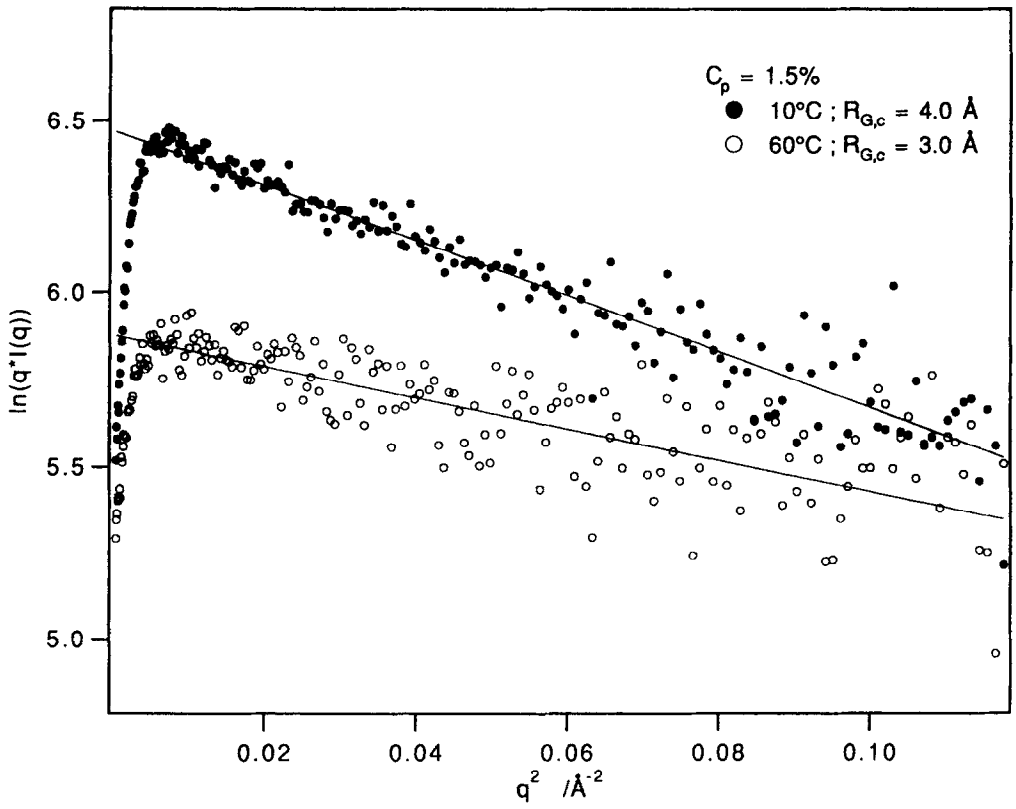

Fig. 2. Cross-sectional Guinier plots ($\ln(q \cdot I(q))$ vs q^2) for SAXS from gellan gum aqueous solution at 10 and 60°C. The concentration is $C_p = 1.5$wt% and the estimated cross-sectional radius of gyration is indicated in the figure.

concentrations (where no gelation takes place) the double helices are formed but are found not to associate further to constitute cross-linking domains.

The distance distribution functions (Fig. 4) were evaluated by the Fourier transformation of the scattering profiles according to the equation,

$$p(r) = (2\pi)^2 \int_0^\infty I(q) \cdot (qr) \cdot \sin(qr) \mathrm{d}q. \quad (2)$$

A peak around 15Å at high temperatures becomes sharp on cooling, and shifts slightly to a larger distance in the gelling systems. Lowering temperature induces a distinctive correlation hole (a negative region in $p(r)$), which is characteristic of an electrostatic interaction. Since the domains composed of several double-stranded chains are formed at lower temperatures, the charges are condensed around the double-stranded portions and electrostatic interaction is considered to be exerted mainly between the newly formed domains by lowering temperature. The first peak (at smaller r) in Fig. 4 may indicate the existence of the domains which are distinguished by higher electron densities from the surrounding. The domains are considered to be composed of single and/or double helices and may contain the associated double helices in the gel state. The shape and size of the domains can be speculated from the peak profile. The shift of the peak position from a shorter to a larger distance on cooling corresponds to the conformational change from a single to a double helix or an association of double helices in the gellan gum solutions of higher concentrations when the gel is formed, since the peak position reflects approximately the cross-sectional radius in the case of a cylindrical object. The length of the cylindrical object is given by the position where the distance distribution function falls to zero,

Table 1. The cross-sectional radius of gyration $R_{G,c}$ and the ratio of the linear mass density at 10°C to that at 60°C, M_L(10°C)/M_L(60°C)

Polymer concentration, %	Cross-sectional radius of gyration		M_L(10°C)/ M_L (60°C)
	60°C, Å	10°C, Å	
1.0	2.7	3.5	1.9
1.5	3.0	4.0	1.8
2.9	2.3	4.7, 5.7 (gel)	2.3, 2.7
5.7	1.8 [80°C]	6.2, 9.5 (gel)	3.8, 5.7

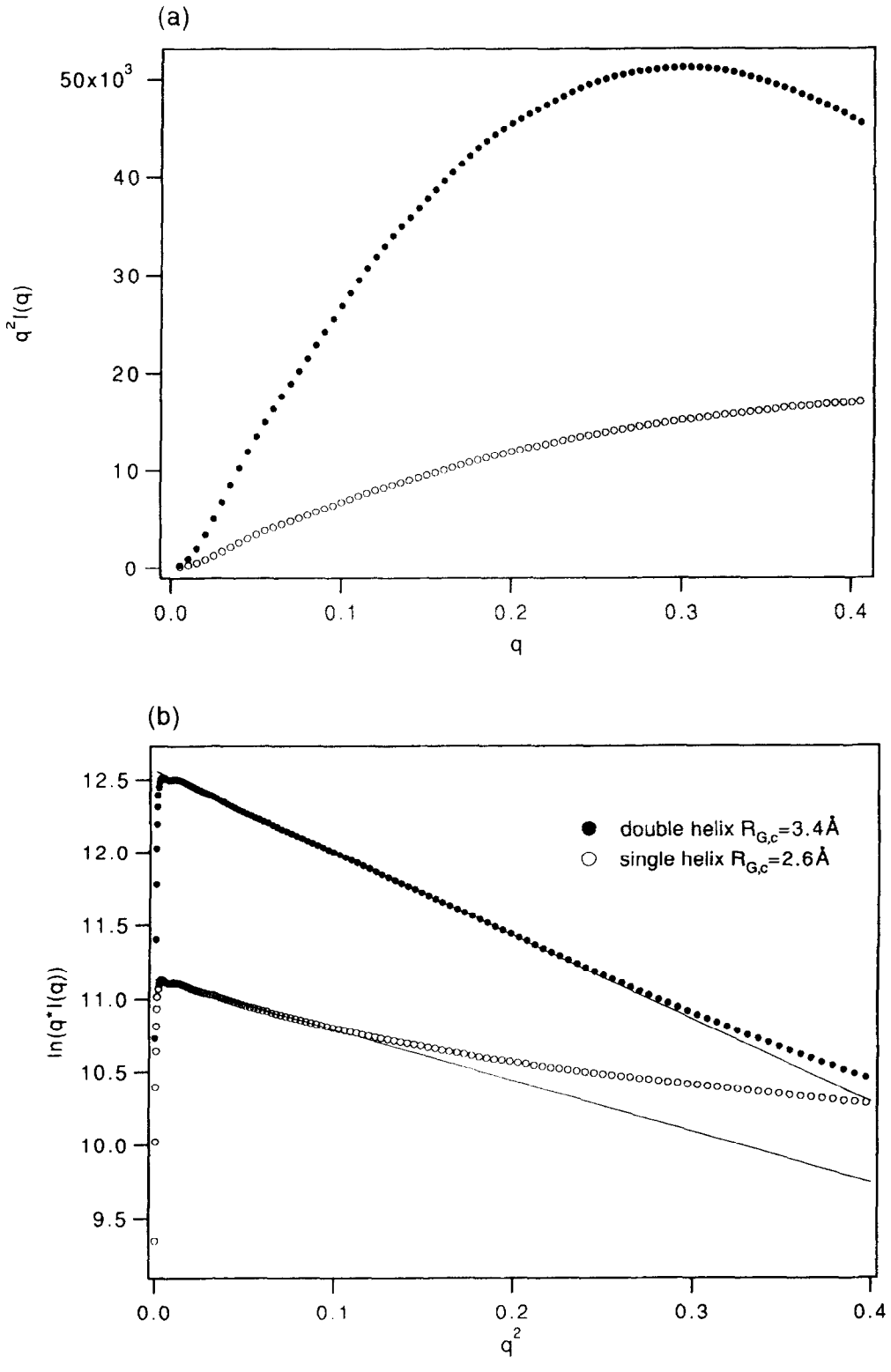

Fig. 3. (a) Kratky plot ($q^2I(q)$ vs q) and (b) cross-sectional Guinier plots ($\ln(q \cdot I(q))$ vs q^2) for SAXS calculated from the gellan gum molecular models in double helix (closed circles) and single helix (open circles).

which is around 50Å at 10°C and is a little shorter at higher temperature. Thus the gellan gum in aqueous solution is speculated to consist of the fragments of single and/or double helices (or associated double helices) of around 50Å in length.

Further analysis of the SAXS data was performed by model-fitting (Guenet, 1992; Fazel *et al.*, 1992). The gellan chains are considered to have a rigid rod-like structure from the scattering profiles. Thus the broken rod model linked by a flexible chain was adopted to

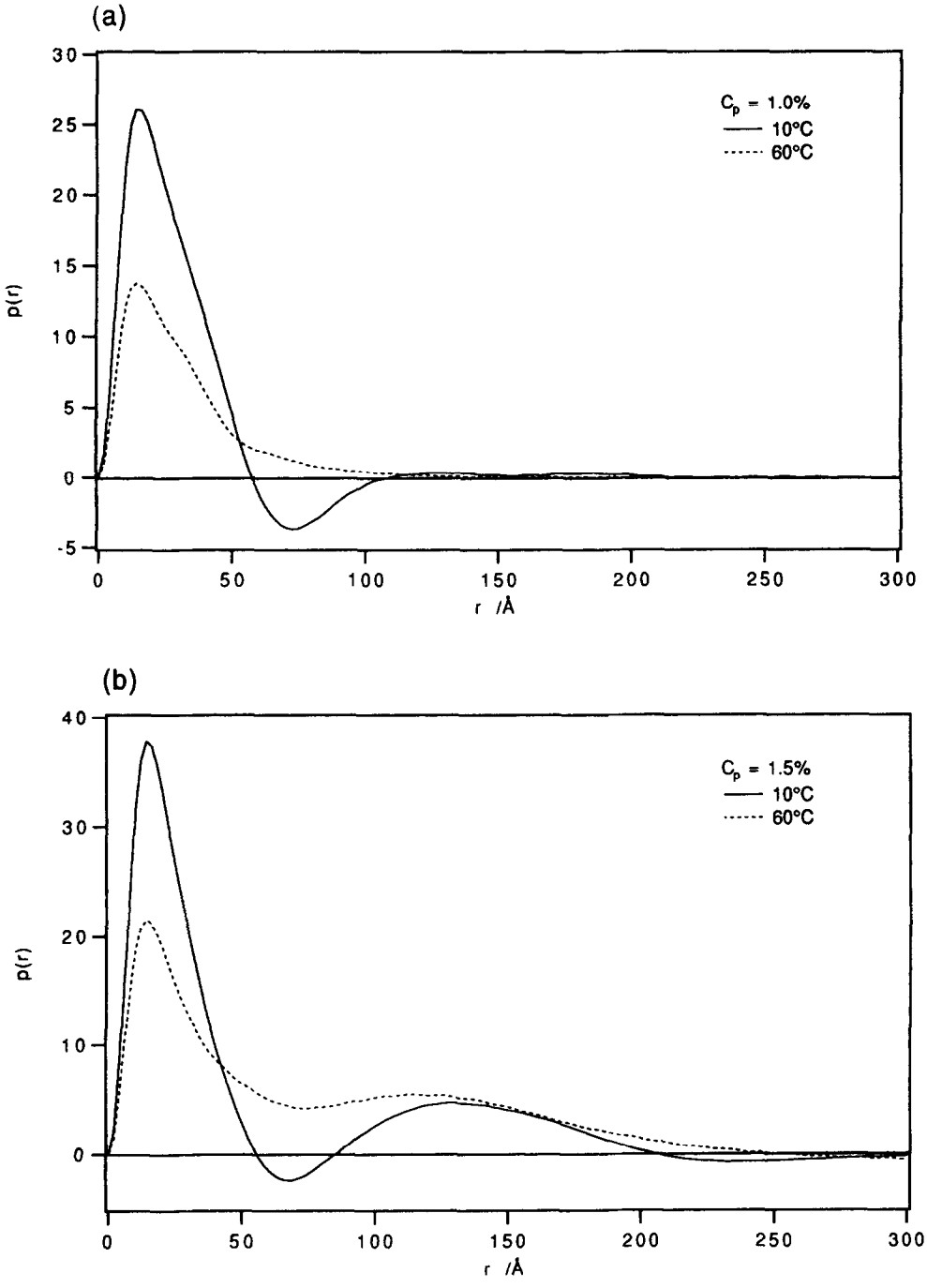

Fig. 4. Distance distribution function evaluated by the Fourier transformation of SAXS intensities from gellan gum aqueous solution. The concentrations and temperatures are indicated in the figure.

simulate the observed SAXS profile according to the following scattering factor

$$P(q) \sim \frac{1}{q^2}\left(\sum_i \pi q w_i M_{Li} \frac{4J_1^2(qR_{ci})}{(qR_{ci})^2} + \text{const.}\right) \quad (3)$$

which takes into account the effect of the cylinder cross-section R_c, and the heterogeneity with regard to the cross-section is considered by introducing the weight fraction w_i of the component i specified by the cross-sectional radius R_{ci} and a linear mass density M_{Li}. Here $J_1(x)$ is the first-order Bessel function. Provided that the interaction is spherical-symmetric, we may introduce the interference $S(q)$ due to the repulsive interaction between domains in the scattering intensity $I(q)$ as

$$I(q) \sim P(q) \cdot S(q) \quad (4)$$

where $S(q)$ is approximately given as

$$S(q) \sim \frac{1}{1 + c \cdot \exp(-\xi^2 q^2)} \quad (5)$$

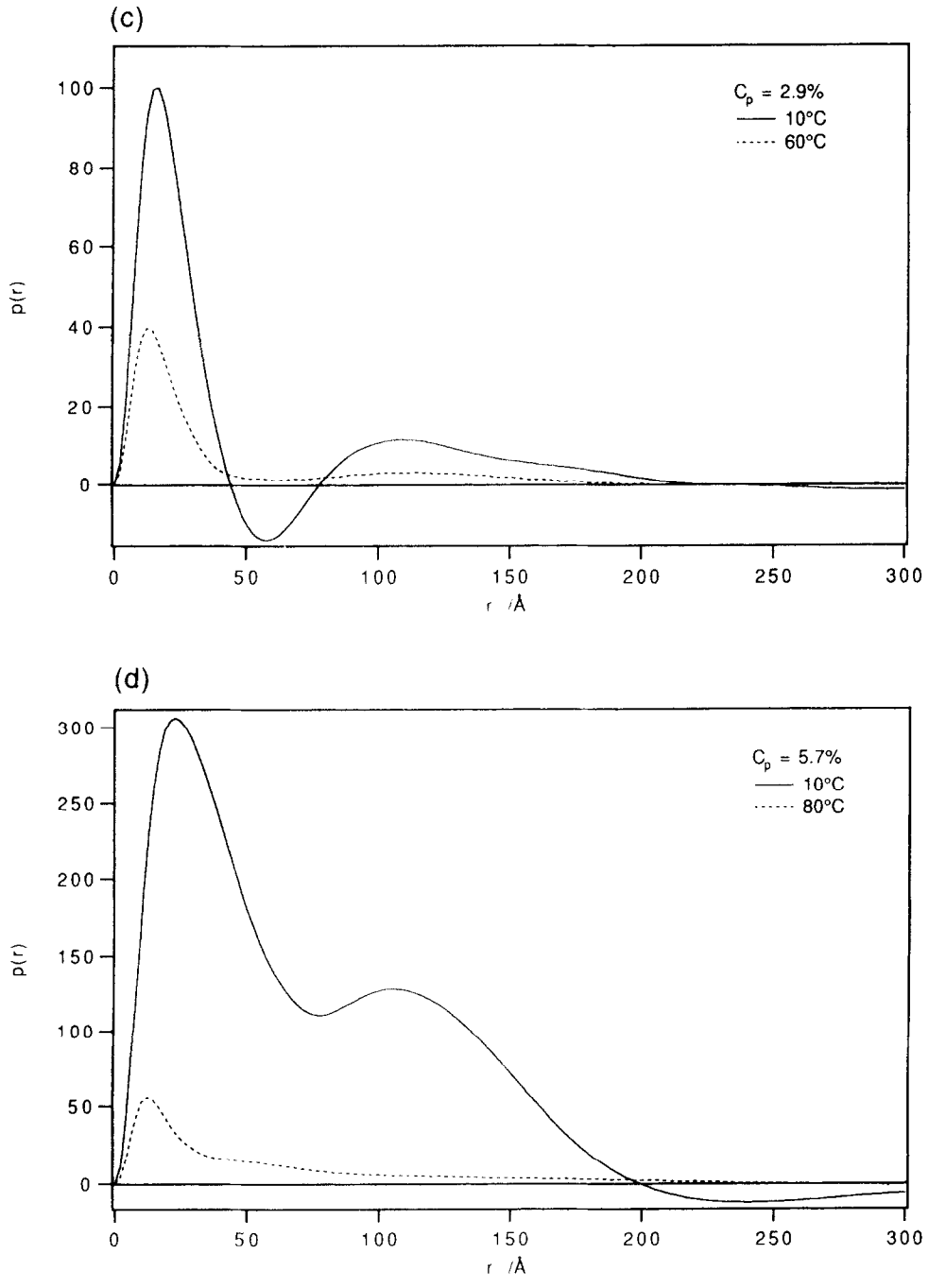

Fig. 4. *Contd.*

which assumes a Gaussian-type interaction potential specified by the correlation length ξ. Here c is an adjustable parameter to take into account the strength of interaction. The observed SAXS was plotted in terms of the Kratky plots ($q^2I(q)$ vs q) as shown in Fig. 5 and fitted according to eqns (4) and (5). The obtained parameters were listed in Table 2, where the simulated values of the cross-sectional radius R_c are found to be almost identical to the values of the cross-sectional radius of gyration $R_{G,c}$ (R_c is given by $\sqrt{2}R_{G,c}$ for a cross-section of homogeneous density) estimated by the cross-sectional Guinier plots. The correlation length of interaction as well as the cross-sectional radius decrease with increasing gellan gum concentration at higher temperature. This is probably due to the unfolding of single helices to random coils, promoted by the cooperative motion of gellan gum chains. As a result, the electric charges are more widely distributed with increasing gellan gum concentrations and consequently the correlation length of interaction is reduced.

Upon cooling, the cooperative chain motion is suppressed and the formation of double helices takes place. Subsequent association of double helices is

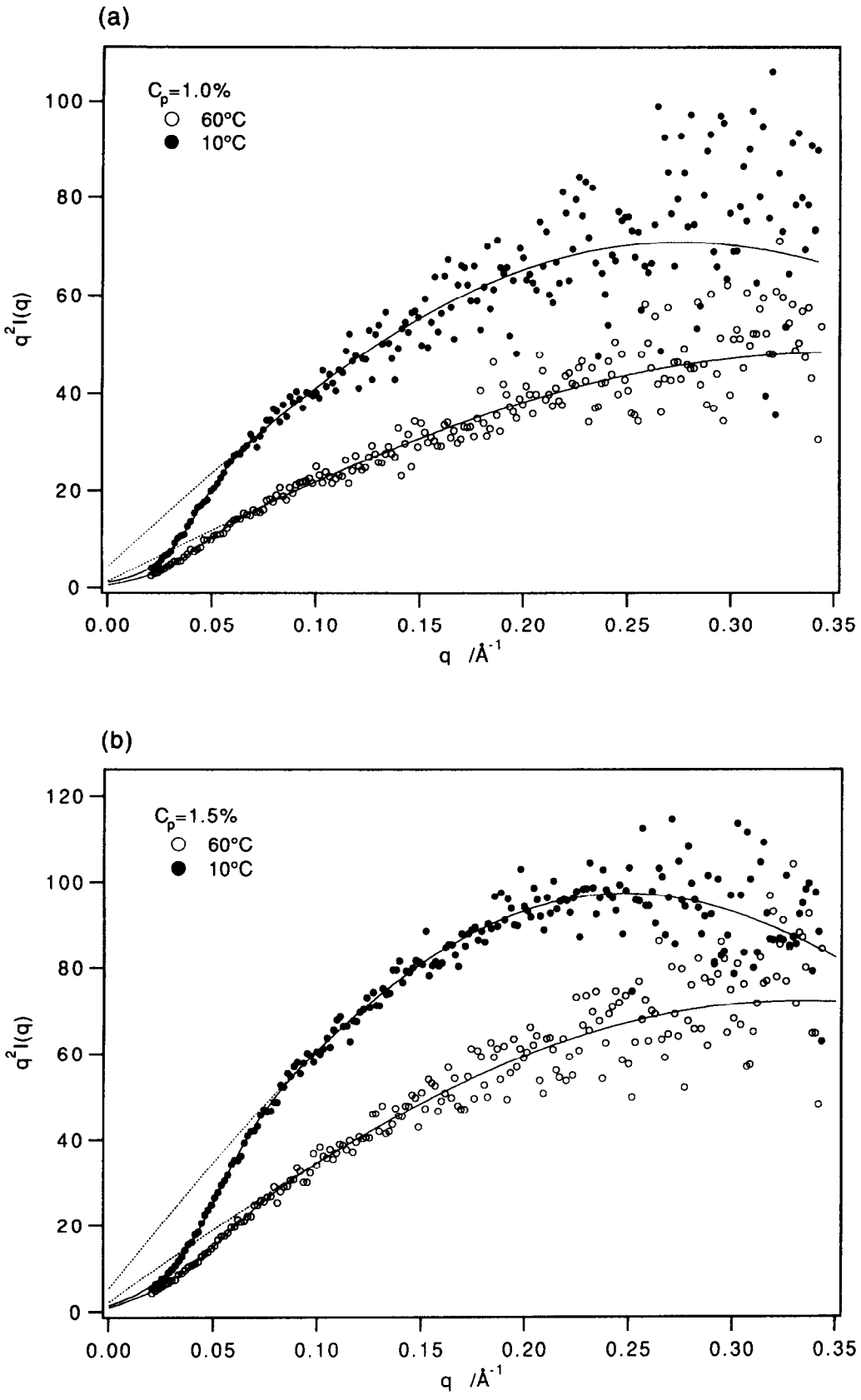

Fig. 5. Kratky plots ($q^2I(q)$ vs q) for SAXS from gellan gum aqueous solution, and the SAXS profile calculated from eqns (4) and (5) (solid line). The broken line indicates the scattering factor $P(q)$. The concentrations and temperatures are indicated in the figure, and the parameters used in the profile calculation are listed in Table 2.

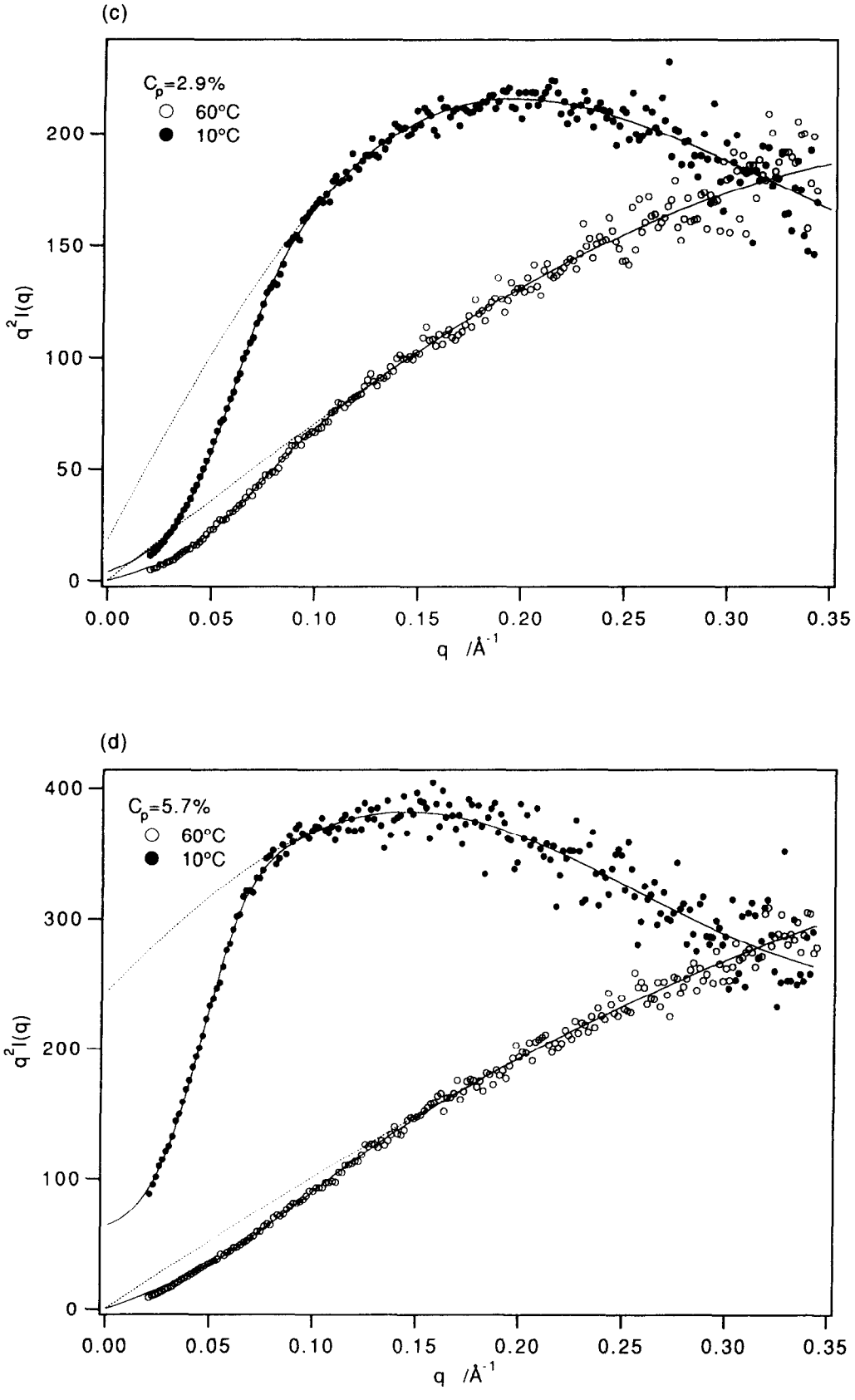

Fig. 5. *Contd.*

Table 2. The cross-sectional radius and the correlation length of interaction

Polymer concentration, %	60°C		10°C	
	R_c, Å	ξ, Å	R_c, Å	ξ, Å
1.0	3.8	31.6	4.9	35.0
1.5	4.1	25.2	5.5	28.3
2.9	3.1	19.9	5.2(0.85), 10.5(0.15)	25.1
5.7	2.4	13.7 [80°C]	9.0(0.92), 12.1(0.08)	28.7

*The values in the brackets denote the weight fraction of the corresponding components (see eqn (3)).

promoted by increasing gellan gum concentration, and a gel is eventually formed. Thus the cross-sectional radius increases with gellan gum concentration, when two components of the cross-sectional radius were formed in the gel state, suggesting some increase in the size distribution of the domains composed of associated double helices. The larger correlation length of interaction than the corresponding values at higher temperatures suggests that the formation of thicker domains causes the condensation of electric charges around domains and results in the larger interaction distance. However, the concentration dependence of the correlation length of interaction is less marked at 10°C, and tends to become negligible upon gelation. The further association of double helices seems to take place so as to maintain the correlation length of interaction rather constant.

CONCLUSION

SAXS is proved to be an efficient method to evaluate the mechanism of gel formation as well as the gel structure in the gellan gum aqueous solutions. The further association of double helices seems to be essential in the gel formation of gellan gum in aqueous solution, while the type of counter ions controls the association of double helices.

ACKNOWLEDGEMENTS

The work was performed under the approval of Photon Factory Advisory Committee (Proposal No. 91-217).

REFERENCES

A special issue of Food Hydrocolloids. (1993). *Food Hydrocolloids*, **7**, 363–447, 457–458.

Carroll, V., Chilvers, G.R., Franklin, D., Miles, M., Morris, V.J. & Ring, S.G. (1983). *Carbohydr. Res.*, **114**, 181–191.

Chandrasekaran, R., Puigjaner, L.C., Joyce, K.L. & Arnott, S. (1988). *Carbohydr. Res.*, **181**, 23–40.

Crescenzi, V., Dentini, M. & Dea, I.C.M. (1986). *Carbohydr. Res.*, **114**, 181–191.

Dentini, M., Coviello, T., Burchard, W. & Crescenzi, V. (1988). *Macromolecules*, **21**, 3312–3320.

Fazel, N., Fazel, Z., Brûlet, A. & Guenet, J.-M. (1992). *J. Phys. II, France*, **2**, 1617–1629.

Grasdalen, H. & Smidsød, O. (1987). *Carbohydr. Res.*, **7**, 371–393.

Guenet, J.-M. (1992). *Thermoreversible Gelation of Polymers and Biopolymers*. Academic Press, London, pp. 89–186.

Jansson, P., Lindberg, B. & Sandford, P.A. (1983). *Carbohydr. Res.*, **124**, 135–139.

Milas, M., Shi, X. & Rinaudo, M. (1990). *Biopolymers*, **30**, 451–464.

Stokke, B.T., Elgsaeter, A. & Kitamura, S. (1993). *Int. J. Biol. Macromol.*, **15**, 63–68.

Yuguchi, Y., Mimura, M., Kitamura, S., Urakawa, H. & Kajiwara, K. (1993). *Food Hydrocolloids*, **7**, 373–385.